Intraseasonal and Seasonally Persisting Patterns of Indian Monsoon Rainfall

V. KRISHNAMURTHY AND J. SHUKLA

Center for Ocean-Land-Atmosphere Studies
Institute of Global Environment and Society, Inc.
Calverton, Maryland
and
School of Computational Sciences
George Mason University
Fairfax, Virginia

June 2005

Corresponding author's address:
V. Krishnamurthy
COLA, IGES
4041 Powder Mill Road, Suite 302
Calverton, MD 20705
E-mail: krishna@cola.iges.org

Abstract

The space-time structure of the active and break periods of the Indian monsoon has been studied using a 70-year long high resolution gridded daily rainfall data over India. The analysis of lagged composites of rainfall anomalies based on an objective categorization of active and break phases shows that the active (break) cycle, with an average life of 16 days, starts with positive (negative) rainfall anomalies over the Western Ghats and eastern part of central India and intensifies and expands to a region covering central India and parts of north India during the peak phase while negative (positive) anomalies cover the sub-Himalayan region and southeast India. During the final stage of the active (break) period, the positive (negative) rainfall anomalies move toward the foothills of the Himalayas while peninsular India is covered with opposite sign anomalies. The number of days on which lows and depressions are present in the region during active and break periods is consistent with the rainfall analysis.

Using multichannel singular spectrum analysis of the daily rainfall anomalies, the seasonal monsoon rainfall is found to consist of two dominant intraseasonal oscillations with periods of 45 and 20 days and three seasonally persisting components. The 45-day and 20-day oscillations are manifestations of the active and break periods but contribute very little to the seasonal mean rainfall. The seasonally persisting components with anomalies of the same sign, and covering all of India, have a very high interannual correlation with the total seasonal mean rainfall. These results support a conceptual model of the interannual variability of the monsoon rainfall consisting of seasonal mean components and a statistical average of the intraseasonal variations. The success in the prediction of seasonal mean rainfall depends on the relative strengths of the seasonally persisting components and intraseasonal oscillations.

1. Introduction

The intraseasonal variation of the Indian monsoon consists of "active" periods of high rainfall and "break" periods of deficient or no rainfall during the summer season [June-July-August-September (JJAS)]. The JJAS seasonal mean rainfall varies from year to year and is known to have strong associations with other global phenomena through the influence of sea surface temperature (SST), snow, and soil moisture (see, e.g., Krishnamurthy and Kinter 2003). Based on model experiments, Charney and Shukla (1981) suggested that a large part of the monsoon variability is due to slowly varying boundary conditions such as the SST and albedo and therefore potentially predictable on a longer time scale. By analyzing 70-year long high-resolution data of observed daily rainfall over India, Krishnamurthy and Shukla (2000) suggested a conceptual model of the interannual variability of the Indian monsoon to consist of a linear combination of a large-scale persistent seasonal mean component and a statistical average of the intraseasonal variations.

The conceptual model put forward by Krishnamurthy and Shukla (2000) is an extension of Charney-Shukla hypothesis and is based on the following results of their study. The dominant mode of the daily rainfall has anomalies of one sign over central India and anomalies of opposite sign over the foothills of the Himalayas in the north and over southeast India. The dominant pattern of the seasonal rainfall anomalies, however, has a large scale spatial pattern with anomalies of the same sign over all of India and persists throughout the monsoon season. Once the seasonal mean anomalies are removed, the nature of the intraseasonal variability of the daily rainfall anomalies is not different from one year to another, and more importantly between drought years and flood years. However, the major drought (flood) years are characterized by the presence of a strong seasonal signature of negative (positive) rainfall anomalies covering all

of India for the entire monsoon season. The large-scale seasonally persistent pattern can be part of the low-frequency components of the monsoon system influenced by the slowly varying land and ocean boundary anomalies. These results and the conceptual model imply that the success in predicting the seasonal mean rainfall over India depends on the relative magnitudes of the intraseasonal component and the seasonally persisting component.

The intraseasonal variation of the Indian monsoon has been found to mainly consist of fluctuations on time scales of 10-20 days and 30-60 days. The 10-20 day variability was observed in the spectra of pressure, cloud cover, rainfall and static stability over the Indian monsoon region by Krishnamurti and Bhalme (1976) and in cloudiness data by Yasunari (1979). These results were based on data covering one to three monsoon seasons. A spectral peak in the 40-50 day range was found in a long record of daily rainfall over India by Hartmann and Michelsen (1989) while several studies (e.g., Yasunari 1979, Lau and Chan 1986) have noted the variability on the same time scale in convection data over a larger monsoon region. The presence of 10-20 day and 30-60 day variability was also found in a principal oscillation pattern analysis of outgoing longwave radiation (OLR) and reanalysis circulation products for 1979-95 by Annamalai and Slingo (2001). They estimated that 10-20 day and 30-60 day fluctuations explain about 25% and 66%, respectively, of the total Intraseasonal variability. However, Goswami et al. (1998), who also found the intraseasonal modes on the same two scales in the reanalysis circulation data, estimated that the two modes explain about 10–25% of the total daily variance.

Most studies associate the intraseasonal variations on the two dominant time scales with the active and break phases of the monsoon. Although rainfall is the most important manifestation of the monsoon variability and the most direct cause of the socio-economic impact of monsoon that is often cited, there has been no study showing a direct correspondence between

the active and break periods observed in the rainfall and the intraseasonal modes noted in other monsoon variables. The presence of the 10-20 day and 30-60 day variability in a long record of the daily rainfall over India has also not been shown previously.

The aforementioned results of Krishnamurthy and Shukla (2000) suggest that the prediction of the seasonal mean monsoon rainfall depends on the relative strengths of the 10-20 day and 30-60 day fluctuations and the component with the seasonal signature that is presumably influenced by boundary forcing. An alternate interpretation of Charney-Shukla hypothesis as to what determines the seasonal mean rainfall suggests that the boundary conditions merely alter the probability distribution function (PDF) of the rainfall to have a bias toward the active or break phase (Palmer 1994). In this scenario, the seasonal mean rainfall is determined by a bimodal PDF of rainfall and depends on the frequency and length of active and break phases. Goswami and Ajaya Mohan (2001) identified a mode of variability in the reanalysis winds at 850 hPa as common to both intraseasonal and interannual time scales and presented an asymmetric bimodal PDF of the intraseasonal mode. They related the bimodality of the PDF to active and break periods defined on the basis of an index of 850 hPa zonal winds over the Bay of Bengal. In an empirical orthogonal function (EOF) analysis of the reanalysis winds at 850 hPa, Sperber et al. (2000) identified the third EOF of the daily winds and the fourth EOF of the seasonal winds as a common mode of intraseasonal and interannual variability, but found no bimodality in the PDF of the principal component (PC) of the intraseasonal mode. Lawrence and Webster (2001) found that the intraseasonal variability of OLR for the period 1975–97 was moderately correlated with the seasonal mean Indian rainfall but was uncorrelated with the seasonal SST anomalies. Singh et al. (1992) found that the intraseasonal variability of the rainfall over India was not related to either the total seasonal rainfall or the El Niño and Southern Oscillation (ENSO).

The above discussion points to an obvious need for clarification of the relation between the intraseasonal variability and the seasonal mean monsoon rainfall over India. The purpose of this paper is to identify the modes of intraseasonal variability and the components with the seasonal signature in the monsoon rainfall. The relation between these components and the JJAS seasonal mean rainfall will be investigated. The space-time structure of the active and break phases of the monsoon will be examined and the correspondence to intraseasonal modes of variability on two dominant time scales will be established. An important aspect of this study is that the results are based on the analysis of a long record of high resolution daily rainfall over India rather than using reanalysis winds or OLR. The results of this paper will strongly support the conceptual model suggested by Krishnamurthy and Shukla (2000) and show that the intraseasonal modes on two different time scales (20 and 45 days) oscillate about seasonally persisting components that are shown to be the main contributors to the seasonal mean rainfall.

The data and methods of analysis used in this study are described in section 2. The life cycles of the active and break periods of the monsoon rainfall are discussed in section 3. Section 4 presents an analysis resolving the daily rainfall over India into two dominant modes of intraseasonal variability and seasonally persisting components. The relation between these components and the seasonal mean rainfall is discussed. Conclusions are provided in section 5.

2. Data and methods

a. Data

The intraseasonal variability of the monsoon is studied in this paper by analyzing gridded daily rainfall data for the period 1901–70. The data originated from observations made by the India Meteorological Department (IMD) at more than 3700 rain gauge stations in India and were

later transformed to a 1° longitude ×1° latitude grid over India by Hartmann and Michelsen (1989). Each grid box in this dataset has observations from several stations for most of the time period. This data set was earlier used by Krishnamurthy and Shukla (2000), who filled missing data points for some of the days by linear interpolation.

Over India and the adjoining Indian Ocean region, the main rain-producing systems are the monsoon trough that moves north-south and the transitory low pressure systems (LPSs). The LPSs are categorized as lows, depressions, cyclonic storms, severe cyclonic storms and hurricanes based on their intensity. The lows (systems with wind speeds up to 9 m s^{-1}) and the depressions (winds in the range 9–17 m s^{-1}) are major contributors to the monsoon rainfall. Most of the LPSs are formed east of 80°E over the Bay of Bengal and move in a northwest direction across central and north India; only a few systems are formed over the Arabian Sea. This study has examined the LPS data consisting of daily location and intensity during the life of each LPS from the compilation of Mooley and Shukla (1987) who followed an objective criterion based on the central pressure to classify the LPSs for the period 1888-1983.

The daily rainfall climatology was calculated as the 70-year mean of the total daily rainfall for each calendar day of the year and was subtracted from the total daily rainfall to obtain the daily rainfall anomaly. The JJAS seasonal rainfall anomaly was computed by averaging the daily values over 1 June to 30 September. The daily rainfall data were converted to 5-day running means to obtain a more coherent analysis without the very high frequency fluctuations.

b. Multi-channel singular spectrum analysis

The dominant spatial patterns of the daily and seasonal monsoon rainfall were earlier found by an EOF analysis of the JJAS rainfall anomalies (Krishnamurthy and Shukla 2000). In

order to identify the temporal variability and to determine the coherent intraseasonal space-time patterns of the rainfall, the method of analysis used in this study is the multi-channel singular spectrum analysis (MSSA). This method has been applied to 700 hPa geopotential heights by Plaut and Vautard (1994) to study the intraseasonal variability in the midlatitudes and was reviewed by Ghil et al. (2002) who cite several studies that have used this method for analyzing variability ranging from intraseasonal to interdecadal time scales. Both these papers provide the mathematical formulation and technical details of MSSA and point out its equivalence to extended EOF (EEOF) analysis. The following brief description of MSSA is based on the discussion of the method by Plaut and Vautard (1994) and Ghil et al. (2002).

EEOF analysis and MSSA are both extensions of the familiar EOF analysis but include temporal lags of spatial data to obtain space-time patterns of variability. The temporal and spectral information obtained by the analysis depends on the length of the time lags. While EEOF analysis includes only a few time lags, MSSA typically includes larger number of lags, sufficient to identify oscillations and trends on the time scale of interest and to extract their temporal and spatial properties. MSSA is applied to a data set consisting of time series of L channels (e.g., points on a grid) given at N discrete times at equally spaced time interval Δt. The analysis involves constructing a covariance matrix of the multi-channel time series at temporal lags ranging from 0 to $M-1$ and diagonalizing the lag-covariance matrix to yield LM eigenvalues and LM eigenvectors (not necessarily distinct). Alternately, the multi-channel time series matrix is augmented with M lagged copies of itself, and a singular value decomposition of the augmented matrix is carried out. The parameter M is called the window length. The eigenvectors are the space-time EOFs (ST-EOFs), each an M sequence of maps, describing space-time patterns of decreasing importance as the corresponding eigenvalues decrease. The

projection coefficients of the data onto the ST-EOFs are the space-time principal components (ST-PCs) of time length $N' = N - M + 1$, and the variance is given by the eigenvalues.

An oscillation in the time series is identifiable when two consecutive ST-PCs with nearly equal eigenvalues are in phase quadrature. The corresponding ST-EOFs in this case are also nearly periodic with the same period and in phase quadrature. The period and spatial pattern of such an oscillation are same as those of the ST-EOFs. It is possible to distinguish oscillations possessing the same spatial patterns but different periods as well as oscillations with same period but with orthogonal spatial patterns. The eigenmodes not associated with oscillatory pairs also provide useful information, particularly about trends and persisting patterns.

The part of the original time series corresponding to a particular eigenmode can be extracted as space-time reconstructed components (RCs) defined by Plaut and Vautard (1994). The RCs are simply projections of the data onto the corresponding M ST-EOFs and are multi-channel (or spatial grid) maps whose time length and sequence are exactly those of the original time series. The sum of all the RCs reproduces the original time series. For an oscillation represented by a pair of eigenmodes, the RC is sum of the individual RCs of the pair. The amplitude $A(t)$ and the phase angle $\theta(t)$ of the oscillation can be determined from the RC using the method provided by Moron et al. (1998). The phase angle θ varies from 0 to 2π for each cycle of the oscillation. The periods of the oscillations resolved by MSSA depend on the choice of the window length M and are estimated to be in the range (M/5, M) (Plaut and Vautard 1994).

c. Space-time frequency spectrum

To investigate whether the rainfall anomaly has components that are propagating, space-time spectral analysis is used. This technique has been used in intraseasonal studies (e.g.,

Wheeler and Kiladis 1999) to identify the spatial scales and the propagation characteristics associated with different frequencies of variability in the data. The space-time domains of the total rainfall anomalies and the RCs from MSSA are converted into wavenumber-frequency domains. This study applies the spectral analysis to data in a domain limited to India to look for propagating waves in north-south and east-west directions as well as standing patterns. The spectra are computed by performing fast Fourier transform of the discrete data in space and time. Because of the limited domain of the data, the gravest mode (wavenumber 1) of this analysis corresponds to the meridional and zonal extent of the data. Pratt (1976) has provided helpful discussion to infer propagation properties from space-time spectra.

3. Life cycles of active and break periods

An objective definition of the active and break periods of the Indian monsoon used in this study is based on the daily rainfall anomalies, similar to the definition by Krishnamurthy and Shukla (2000). From an EOF analysis of standardized daily rainfall anomalies for JJAS 1901–70, the principal component (PC) corresponding to the first EOF is computed. The active (break) period is identified as the period when the daily PC 1 is above (below) a certain positive (negative) threshold for at least five consecutive days, the threshold being one-half of the standard deviation of PC 1. The daily PC 1 has very high correlation with the daily rainfall anomalies area averaged over India (Krishnamurthy and Shukla 2000). For JJAS 1901–70, this criterion yields 217 active periods and 217 break periods with the longest active and break periods extending to 32 and 30 days respectively.

a. Composites of rainfall and low pressure systems

The active and break composites of daily rainfall anomalies were constructed by averaging the anomalies over all active and break days, respectively, during JJAS 1901–70. The active composite in Fig. 1a shows positive anomalies over a large part of India and negative anomalies near the eastern part of the foothills of the Himalayas and over the southeastern part of India. The Western Ghats is the region of maximum rainfall anomalies with more than 8 mm day^{-1} while large anomalies in the range 4–8 mm day^{-1} occur across Central India in a band that is tilted in northwest-southeast direction. The negative anomaly region near the Himalayas and the eastern Indian states has minimum values below −8 mm day^{-1} while in the southeast the minimum is about −2 mm day^{-1}. The break composite of the rainfall anomalies (Fig. 1b) has a structure similar to that of the active composite but with anomalies of opposite sign.

The composites of LPS-days for active and break periods defined above were also constructed for JJAS 1901–70, and the composites for depression-days are shown in Figs. 1c and 1d. An LPS-day here refers to one day on which the system of a particular category (e.g., low or depression) exists in the Indian monsoon region. The mean life of the LPS formed over the Bay of Bengal is 5 days whereas it is 3 days for those formed over land and over the Arabian Sea (Mooley and Shukla 1987). Therefore, a single LPS is represented by several LPS-days (equal to its life) in the composites following its evolution. The composites in Figs. 1c and 1d show the locations of all the depression-days during active and break periods, respectively. There are 807 depression-days in the active composite (Fig. 1c) and 110 depression-days in the break composite (Fig. 1d), showing clearly that most depression-days during the monsoon season are associated with the active periods. Most of the depression-days in the active period (Fig. 1c) are located in the region of maximum rainfall (Fig. 1a) and extend across the entire central India.

The maps containing the trajectories of all the depressions during this period provided by Mooley and Shukla (1987) show that the active composite in Fig. 1c is associated with depressions formed mostly over the Bay of Bengal and over land and moving in west-northwest direction parallel to the axis of the monsoon trough. Such movement of the depressions is consistent with the northwest-southeast tilt in the rainfall bands of the active composite (Fig. 1a). The depression-days of the break composite (Fig. 1d) are mostly located in or near the positive rainfall anomaly in the sub-Himalayan region shown in the rainfall composite (Fig. 1b). A remarkable difference between Figs. 1c and 1d is the location of the depressions. During the break phase, the locations of the depressions are clearly to the north of the locations during the active phase. The depression-days of the break composite occur when the monsoon trough has moved toward the foothills of the Himalayas. The composites of low-days were also examined (not shown) and found to consist of 793 and 397 low-days for the active and break periods, respectively, and show spatial structures similar to the composites of the depression-days shown in Figs. 1c and 1d. These LPSs do not contribute to the heavy rainfall along the Western Ghats, which are influenced more by the quasi-stationary mid-tropospheric disturbances and topography-related off-shore vortices.

b. Evolution of active and break periods

Lagged composites of daily rainfall anomalies with respect to the midpoints of the active and break periods were constructed to study the evolution of the spatial structure of the rainfall during the lives of the active and break phases. The lagged active composites for lags ranging from −10 to +12 days at intervals of two days are shown in Fig. 2 where lag 0 refers to the midpoint of each active period (of varying length) during JJAS 1901–70. On the average, the

active period lasts for about 16 days starting with positive rainfall anomalies appearing in the Western Ghats while central India is covered with weak negative rainfall anomalies (lag −8). At lag −6, the rainfall over the Western Ghats intensifies and positive anomalies appear over the east coast while most of India north of about 22°N is covered with weak negative anomalies. During the next four days (lags −4 and −2 composites), the region of positive anomalies expands over central India with increased intensity of rainfall and negative anomalies are established over southeast India and the sub-Himalayan region in the north. At the peak of the active period (lag 0 composite), all of central India and the Western Ghats are covered with strong positive rainfall anomalies and the negative anomalies near the foothills of the Himalayas have also intensified. Over the next four days (lags +2 and +4 composites), the rainfall weakens over the Western Ghats and the eastern part of central India while the maximum rainfall occurs over the western part of central India accompanied by slightly increased rainfall over north India. During the subsequent four days (lags +6 and +8 composites), the positive rainfall anomalies weaken and move northward and closer to the foothills of the Himalayas while the peninsular region (south of about 20°N) is covered with weak negative rainfall anomalies.

The lagged break composites (figure not shown) look very much similar to the active composites in Fig. 2 but with rainfall anomalies of opposite sign and show that negative rainfall anomalies that develop over the Western Ghats and the east coast intensify and cover most of India except for the positive anomaly regions of southeast India and the sub-Himalayan region in about eight days. The negative anomalies weaken and move northward toward the foothills of the Himalayas while positive anomalies develop over the peninsular region during the subsequent eight days. The average break phase is thus an opposite image of the active phase.

The lagged active and break composites of the LPS-days were also examined (figure not shown). The lagged active composites show the spatial extent and the number of LPS-days (both lows and depressions) consistent with the positive rainfall anomalies shown for different lags in Fig. 2. However, these LPS do not account for the positive anomalies over the Western Ghats. The lagged break composites of LPS-days show very few low-days and depression-days during most of the break phase, especially from lag −4 to lag +6.

c. Area averaged rainfall and relation to seasonal rainfall

A widely used measure of the Indian monsoon is the area averaged rainfall over India (land region); such an average of rainfall anomalies will be referred to as the Indian monsoon rainfall (IMR) index. The lagged active and break composites of the IMR index for JJAS 1901–70 are shown in Fig. 3a. The lagged active composites of the IMR index, for example, are simply the area averages of the rainfall anomaly maps shown in Fig. 2a but plotted in Fig. 3a at one day interval for lags ranging from −22 to +22 days. The IMR index also indicates that active (break) phase, on the average, lasts from lag −8 to lag +8 when the area averaged Indian rainfall anomaly is positive (negative) with a sharp increase (decrease) to a peak value of about 2.7 (−2.2) mm day^{-1} (Fig. 3a). The lagged active and break composites of the total number of depression-days during 1901–70 shown in Fig. 3b are consistent with the composites of IMR index in Fig. 3a. The total number of depression-days reaches a peak value of about 97 during the active phase whereas it goes down to about 5 during the peak of the break phase.

From the variation of the IMR index seen in Fig. 3a, the active and break phases can be considered as fluctuations about a mean value for the JJAS seasonal rainfall. The lagged active and break composites of the IMR index were also constructed separately for strong and weak

monsoon years, as shown in Fig. 4. The eight strong and eight weak monsoon years selected for this purpose are exactly the same as those defined by Krishnamurthy and Shukla (2000), and the JJAS seasonal rainfall anomalies averaged over strong and weak years separately are plotted in Fig. 4. The composites in Fig. 4 show that while the active and break phases fluctuate about the average JJAS seasonal anomaly of 1.07 mm day^{-1} during strong monsoon years they fluctuate about the average of −1.22 mm day^{-1} during weak monsoon years. For the entire life cycle of the active and break phases, strong monsoon years have a persistent rainfall anomaly of about 2 mm day^{-1} higher compared to weak monsoon years. This result supports the conceptual model of Krishnamurthy and Shukla (2000) which suggests that the active and break phases are fluctuations about seasonally persisting components that vary on interannual time scale.

4. MSSA of rainfall anomalies

To resolve the oscillations and persisting signals present in the monsoon variability, MSSA was applied to daily Indian rainfall anomalies for the period 1901–70 following the method detailed by Plaut and Vautard (1994) and Moron et al. (1998). Similar to the EOF analysis of the same data for JJAS months (equivalent to MSSA with M=1) by Krishnamurthy and Shukla (2000), MSSA was carried out using daily rainfall anomalies for 122 days of JJAS of each year with a lag window length M = 61 days. With these specifications and ensuring that no discontinuous data enter into the lagged data during JJAS of each year, each ST-PC is 62 days long each year and each ST-EOF consists of maps in a sequence of 61 lags. The space-time RC of each eigenmode was computed for all 122 days of JJAS of each year corresponding to the exact sequence of the original time series. According to the estimate of Plaut and Vautard (1994), the analysis of this study can expect to distinguish oscillations with periods in the range

of 12 to 61 days. The analysis was repeated with M = 51 and 71 days (using data longer than JJAS for latter case) and the results were found to be similar to those with a 61-day window. Consistent results were also obtained with the data filtered by retaining the first ten modes of a spatial EOF analysis. This paper will discuss the analysis of full data with M = 61 days.

a. Eigenmodes

The eigenvalue spectrum from the MSSA of daily rainfall anomalies is shown in Fig. 5a with the first 30 eigenvalues plotted as percentage fractions of the total variance. It appears that the eigenvalues of order 9 onward are close to reaching the noise level. The first seven eigenmodes were found to be most relevant to describe the dominant modes of the intraseasonal variability of the monsoon rainfall, and explain about 22.2% of the total variance. The eigenmode pairs with almost equal eigenvalues are 1–2, 3–4 and 6–7 as seen in Fig. 5a. However, using the criteria for identifying two consecutive eigenmodes to form an oscillatory pair as specified by Plaut and Vautard (1994) (also see section 2), it is found that pairs 1–2 and 6–7 are oscillatory whereas the pair 3–4 is not. Therefore, eigenmodes of order 3, 4 and 5 emerge as non-oscillatory. The approximate power spectra of the ST-PCs of the first seven eigenmodes are shown in Fig. 5b. The pair 1–2 has a well defined peak at 45 days whereas the pair 6–7 has peaks at about 20 days. The modes 3, 4, and 5 have most of the power in their spectra toward the red part indicating that the components are trends or persisting signals although weak variability associated with peaks close to 30 days are also visible. The wavenumber-frequency spectra of these modes will be discussed later to get a more accurate understanding of the spectral properties.

b. 45-day and 20-day oscillations

After computing the RCs for the first seven modes, the phase angle and the amplitude of the oscillatory pairs 1–2 and 6–7 were determined. Denoting the RC of mode i as $R(i)$ and $R(i)+R(j)$ as $R(i,j)$, the reconstructed oscillations 1–2 and 6–7 (oscillatory parts of the total rainfall anomaly) are the sums $R(1,2)$ and $R(6,7)$, respectively. The daily phase angle θ of the two oscillations and the corresponding RCs at a particular channel (grid point at 77°E and 20°N) for JJAS 1952 and 1955 (randomly selected channel and years as examples) are shown in Fig. 6 along with the IMR index of the daily total rainfall anomaly. The oscillations $R(1,2)$ and $R(6,7)$ are not perfectly periodic but capture the variations in the daily rainfall at, respectively, 45 day and 20 day time scales. The difference in the fraction of total variance explained by $R(1,2)$ (10.1%) and $R(6,7)$ (3.7%) is also evident in the amplitudes of the RCs plotted in Fig. 6.

The space-time structure of the 45-day and 20-day oscillations can be visualized by constructing composites of $R(1,2)$ and $R(6,7)$ based on the phase angle θ of the respective oscillation. The interval $(0, 2\pi)$ in which θ varies is divided into eight equally spaced intervals such that $(k-1)\pi/4 \le \theta(t) < k\pi/4$ with $k = 1, \ldots, 8$. The phase k composite is constructed by averaging the RC over all instances of the oscillation in phase k. The phase composites were constructed separately for the two oscillations.

The composites of $R(1,2)$ for the phases of the oscillatory pair 1–2 shown in Fig. 7a reveal an average oscillatory cycle consisting of active and break phases with a period of about 45 days. Each phase lasts about 5-6 days. The phase 1 composite shows the developing stage of the active period with positive rainfall anomalies over most of the peninsular region with maximum values over the Western Ghats. The active phase gets established and peaks in phase 2 and 3 composites with strong positive rainfall anomalies over central India and the Western

Ghats and negative anomalies near the foothills of the Himalayas and over southeast India. The final stage of the active phase with positive rainfall anomalies weakening and moving closer to the foothills of the Himalayas is seen in the phase 4 composite. Similar onset, establishment and the final stages of the break period are seen in phase 5 through 8 composites which are almost exactly the opposite of phase 1 through 4 composites respectively. The space-time structure of the active phase of this 45-day oscillation follows a sequence similar to the life cycle of the active phase shown in Fig. 2 using composites based on active days defined by actual rainfall anomalies. The only difference lies in the period of the cycle between the two composites.

The phase composites of $R(6,7)$ for the phases of the oscillatory pair 6–7 are shown in Fig. 7b. The 6–7 oscillation also consists of a cycle of active and break phases similar to that of the 1–2 oscillation (shown in Fig. 7a) except that the average period is about 20 days and the amplitude is about half that of the 1–2 oscillation.

Similar phase composites of the number of depression-days also confirm the space-time structure of the 45-day and 20-day oscillations. There are 557 depression-days during phases 2 and 3 of the active phase of covering the Central India and part of the Bay of Bengal (Fig. 8a) while there are only 182 depression-days during phases 6 and 7 of the break period (Fig. 8b) in the 1–2 oscillation. Similar composites of the 6–7 oscillation show 472 depression-days during the active phase (Fig. 8c) and 262 depression-days during the break phase (Fig. 8d). The phase composites in Fig. 8 have good resemblance to the active and break composites of the depression-days based on the total rainfall anomalies shown in Fig. 1.

The phase composites were also constructed using a shorter phase interval of $\pi/12$ to examine the evolution of the oscillation on a finer time scale. The phase composites of the total rainfall anomalies were also examined for the two oscillations and were found to possess spatial

structure similar to and magnitudes comparable to the composites of the corresponding RC. For a compact display of one complete phase cycle of each oscillation, the area averages of the phase composites of $R(1,2)$ and $R(6,7)$ over India (similar to the IMR index) are plotted in Fig. 9a. While the average cycles of both $R(1,2)$ and $R(6,7)$ consist of well defined active and break phases, the peak amplitudes of $R(1,2)$ and $R(6,7)$ are about 1.2 mm day^{-1} and 0.6 mm day^{-1} respectively. The amplitude of $R(1,2)$ attains its peak value at phase $\pm\pi/2$ whereas it happens at $\pm 2\pi/3$ for $R(6,7)$. The phase composites of the depression-days (Fig. 9b) show depression activities consistent with the composites of RCs (Fig. 9a) with most of the depression-days occurring during the active period. The phase composites of the total rainfall anomaly for the two oscillations (Fig. 9c) are very close to those of the RCs (Fig. 9a) confirming that the two oscillations represent the dominant modes of intreaseasonal variability. Comparing with the composites in Fig. 2 and 3, it is evident that $R(1,2)$ and $R(6,7)$ together contribute considerably to the amplitude of the total rainfall anomaly during active and break periods. The combination of $R(1,2)$ and $R(6,7)$ plays a dominating role in determining the phase and length of the active and break periods represented in Figs. 2 and 3. The actual contribution of these two oscillatory modes to the total rainfall anomalies during the monsoon season will be discussed next.

c. Seasonal components

The seasonal mean properties of the first seven eigenmodes of the MSSA will now be discussed to reveal the relative roles of these modes in determining the seasonal mean rainfall. It is necessary to first find the relative contributions of the seven modes to the daily total rainfall anomalies during the active and break phases. For the kind of analysis performed in this study, the non-oscillatory modes 3, 4 and 5 do not show much difference among themselves. The

distinction may lie in what factors (e.g., external forcing) are responsible for producing these components. Therefore, further discussion will consider the RCs of the modes 3, 4 and 5 together and will focus on the sum $R(3)+R(4)+R(5)$, denoted as $R(3,4,5)$. Similar to the composites of the total rainfall anomalies shown in Fig. 1, the active and break composites of daily $R(1,2)$, $R(3,4,5)$ and $R(6,7)$ were constructed using the criterion for active and break periods specified in section 3. The difference between the active and break composites of the RCs and the total rainfall anomaly are shown in Fig. 10a. The composite of the total anomaly in Fig.10a is simply the difference between the active and break composites shown in Figs. 1a and 1b. The daily composites of the components shown have spatial structure similar to that of the total anomaly but with different magnitudes. The component $R(1,2)$ has about twice the magnitude of $R(6,7)$, but the two oscillations together contribute more than $R(3,4,5)$ to the total rainfall anomaly.

To investigate if any of the eigenmodes contain seasonal signature and to determine if the oscillatory modes 1–2 and 6–7 fluctuate about a seasonal signal, JJAS seasonal means of the RCs were computed. The strong and weak monsoon year composites of the JJAS seasonal mean $R(1,2)$, $R(3,4,5)$ and $R(6,7)$ were constructed using the same compositing years used in section 3c. The difference between strong and weak composites of the RCs and the total seasonal rainfall anomaly are presented in Fig. 10b. The seasonal means of $R(1,2)$ and $R(6,7)$ are negligible (note the scale of each composite) although $R(6,7)$ has at least the same sign and somewhat similar spatial structure as those of the total anomaly. On the other hand, $R(3,4,5)$ has close spatial resemblance to the total anomaly with comparable magnitude. The daily and seasonal composites in Fig. 10b strongly indicate that the 45-day and 20-day oscillations fluctuate about a seasonal signal represented by $R(3,4,5)$.

To quantify the seasonal behavior of the components for the entire period of 1901–70, the area averages of the JJAS seasonal means of $R(1,2)$, $R(3,4,5)$ and $R(6,7)$ over India (like IMR index) were computed. The time series of the RCs are shown in Fig. 11 along with that of the total rainfall anomaly (seasonal IMR index). The seasonal means of $R(1,2)$ and $R(6,7)$ are very small for the entire period. While $R(1,2)$ has insignificant negative correlation (–0.14) with the total anomaly, $R(6,7)$ has a small positive correlation (0.36). However, $R(3,4,5)$ has the same magnitude as that of the total rainfall anomaly, and the correlation between them is also very high (0.83).

The daily variation of the oscillatory modes and the seasonally persisting components were examined for all years. Two particular years that will be discussed will serve as good examples of the behavior of the components found in the detailed examination. The selected years are the weak monsoon of 1918 and the strong monsoon of 1959 for which the JJAS seasonal means of $R(1,2)$, $R(3,4,5)$, $R(6,7)$ and the total rainfall anomaly are plotted in Fig. 12. The total anomaly is strongly negative (positive) over most of India west of 85°E for 1918 (1959). These structures are also present in the maps of $R(3,4,5)$ with comparable magnitude. However, $R(1,2)$ and $R(6,7)$ have magnitudes an order less compared to the total seasonal anomaly and bear no spatial resemblance to the total anomaly.

The daily variations for 1918 and 1959 are shown with the area averages of the same components over India in Fig. 13. For most of the season, the total anomaly and $R(3,4,5)$ vary with strong negative (positive) anomalies during 1918 (1959), while both $R(1,2)$ and $R(6,7)$ fluctuate about zero on the time scales of their respective periods. Clearly, $R(3,4,5)$ possesses a persisting seasonal signature that characterizes the weak and strong years. During 1959, $R(3,4,5)$

also shows a mixed variation on the time scale of about 30 days. However, the MSSA did not resolve an oscillation on the 30-day time scale.

d. Propagation

The propagation characteristics of the components may be seen from the frequency-wavenumber spectra shown in Fig. 14. The meridional spectra were calculated for $R(1,2)$, $R(3,4,5)$ and R(6,7) averaged between 68°E and 96°E over the latitude domain 8°–32°N to provide information about north-south propagation. For east-west propagation, the RCs were averaged between 8°N and 32°N and the spectra were obtained for the longitude domain 68°E–96°E. The spectra were computed for each year separately and then averaged over the period 1901–70.

The spectra of $R(1,2)$ in Figs. 14a and 14b indicate that oscillation 1–2 shows northward as well as eastward propagation with a 45-day period. However, the oscillation 6–7 is a propagating wave in the northward and westward direction with a period of 20 days as inferred from the spectra of $R(6,7)$ in Figs. 14c and 14d. In Fig. 14, wavenumber 1 corresponds to the domains 8°–32°N and 68°E–96°E, respectively, for the meridional and zonal spectra. The 45-day oscillation reflects the movement of the monsoon trough in the southwest-northeast direction whereas the 20-day oscillation represents the westward movement of the LPS such as lows and depressions while embedded in the monsoon trough.

The redness in the spectra of $R(3,4,5)$ in both Figs. 14e and 14f indicates that a standing pattern covering entire India with either positive or negative rainfall anomaly persists throughout the season. However, the spectra also exhibit a weaker component that varies on 30-day time

scale possibly as a combination of stationary mode and a northeast-propagating mode with the same sign of anomaly over entire India.

5. Summary and conclusions

By analyzing 70-year long observed daily rainfall data over India, this study has found that rainfall over India during the monsoon season consists of intraseasonal oscillations on different time scales fluctuating about seasonally persisting components. It was also found that the life cycle of the active (break) period of the monsoon lasts about 16 days on the average and starts with positive (negative) rainfall anomalies over the Western Ghats and eastern part of Central India. The positive (negative) rainfall anomalies intensify and cover all of central India and parts of north India while negative (positive) anomalies are established over the sub-Himalayan region and over southeast India during the subsequent evolution of the active (break) period. After the peak phase, the rainfall anomalies move northeast toward the foothills of the Himalayas with diminished intensity while anomalies of opposite sign develop over the entire peninsular region. The lagged composites of the averaged rainfall anomalies for strong and weak monsoon years showed that the active and break phases for any year fluctuate about the seasonally persistent mean anomaly for that year. The number of days when low pressure depressions exist was found to be about eight times more during the active period than during the break period and showed consistent variation with the rainfall anomalies. The dramatic difference in the number and location of the depressions between Figs. 1c and 1d is the basis for an important but yet to be resolved question whether the active and break phases are caused by the variation in the formation of monsoon depressions or whether the difference in large-scale flows during the active and break periods cause the variation in formation of the depressions.

The MSSA of daily rainfall anomalies showed that the intraseasonal monsoon variability consists of two dominant oscillations with periods of 45 and 20 days. The active and break periods of the monsoon are direct manifestations of these two oscillations. Each mode goes through an active phase and a break phase during one period of oscillation following the same sequence of spatial structure of active and break periods described in the previous paragraph. The amplitude of the 45-day oscillation is about twice that of the 20-day oscillation. While the 45-day mode exhibits northeast propagation, the 20-day oscillation shows northwest propagation. The oscillations are associated with the number of lows and depressions varying in a manner consistent with active and break periods. The two oscillations play a major role in determining the length and phase of the active and break periods and contribute considerably to the daily rainfall anomalies during those periods.

The 45-day and 20-day oscillations, however, make almost no contribution to the seasonal mean rainfall. Three other eigenmodes from MSSA were identified as components with seasonal signature. The seasonal means of the three seasonal components have very high interannual correlation with the seasonal mean of the total rainfall anomaly. The dominant space-time structure of the seasonal component consists of anomalies of the same sign covering almost entire India and persisting throughout the monsoon season, as revealed by MSSA and wavenumber-frequency spectra. The seasonal components also include a weak 30-day variation that possibly involves the amplitude variation of a standing pattern that covers India with anomalies of the same sign. The 30-day variation needs further examination by isolating it using some filtering process as MSSA does not resolve it as an oscillatory component.

The results of this study from lag composite analysis and MSSA of daily rainfall provide further support to the conceptual model suggested by Krishnamurthy and Shukla (2000) that

seasonal mean monsoon rainfall anomalies consist of a large scale seasonally persistent component and regional intraseasonal fluctuations. Consistent with the conceptual model, the seasonal rainfall over India is a combination of 45-day and 20-day oscillations fluctuating about large-scale components that persist with same sign throughout the season. It must be noted that only the daily climatology was removed from the data before all the analyses were performed. The conceptual picture was clearly evident in the daily variation of these various components shown for particular years of strong and weak monsoon. The insignificant contributions of the 45-day and 20-day oscillations to the seasonal mean rainfall and the presence of seasonally persisting component further confirm the earlier result of Krishnamurthy and Shukla (2000) that the seasonal mean rainfall is not determined by a bias in the PDF of rainfall toward active or break phase.

The implication of these results for the predictability of the seasonal mean monsoon rainfall is significant. If the seasonally persisting components make relatively large contribution to the seasonal mean rainfall and are related to slowly varying boundary forcings or other low frequency global circulations, the seasonal rainfall anomaly over India may be more predictable. Further work should explore the relation between the boundary forcings, such as SST, soil moisture and snow cover, and the seasonally persisting components of the rainfall. Although the intraseasonal oscillations are found to be small contributors to the seasonal mean rainfall, they are extremely important in determining regional rainfall anomalies. It is also worth investigating to know what kind of influence the boundary anomalies have on the 45-day and 20-day oscillations.

Similar analysis of daily OLR and circulation variables will be helpful to understand the dynamics associated with the intraseasonal modes and the seasonally persisting components of

the rainfall. Some studies (e.g., Sikka and Gadgil 1980) have suggested that the active and break periods of the monsoon rainfall over India are associated with the northward propagation of convection zones from the equatorial Indian Ocean to the Indian land region. The analysis of OLR over the monsoon region including the Indian Ocean can help in testing the hypothesis of northward movement of convection. The results of the analysis of OLR and circulation variables over the Indian monsoon region will be presented in another paper.

Acknowledgments

This research was supported by grants from the National Science Foundation (0334910), the National Oceanic and Atmospheric Administration (NA040AR4310034), and the National Aeronautics and Space Administration (NNG04GG46G). The authors thank Rameshan Kallumal for helpful discussions.

References

Annamalai, H., and J. M. Slingo, 2001: Active/break cycles: diagnosis of the intraseasonal variability of the Asian summer monsoon. *Climate Dyn.*, **18,** 85–102.

Charney, J. G., and J. Shukla, 1981: Predictability of monsoons. *Monsoon Dynamics*, J. Lighthill and R. P. Pearce, Eds., Cambridge University Press, 99–109.

Ghil, M., M. R. Allen, M. D. Dettinger, K. Ide, D. Kondrashov, M. E. Mann, A. W. Robertson, A. Saunders, Y. Tian, F. Varadi, and P. Yiou, 2002: *Rev. Geophys.*, **40(1),** 1003, doi:10.1029/2000RG000092.

Goswami, B. N., and R. S. Ajaya Mohan, 2001: Intraseasonal oscillations and interannual variability of the Indian summer monsoon. *J. Climate*, **14,** 1180–1198.

Goswami, B. N., D. Sengupta, and G. Suresh Kumar (1998): Intraseasonal oscillations and Interannual variability of surface winds over the Indian monsoon region. *Proc. Indian Acad. Sci. (Earth & Planet. Sci.)*, **107,** 1–20.

Hartmann, D. L., and M. L. Michelsen, 1989: Intraseasonal periodicities in Indian rainfall. *J. Atmos. Sci.*, **46,** 2838–2862.

Krishnamurthy, V., and J. L. Kinter III, 2003: The Indian monsoon and its relation to global climate variability. *Global Climate*, X. Rodó and F. A. Comín, Eds., Springer-Verlag, Berlin, 186–236.

Krishnamurthy, V., and J. Shukla, 2000: Intraseasonal and interannual variability of rainfall over India. *J. Climate*, **13,** 4366–4377.

Krishnamurti, T. N., and H. N. Bhalme, 1976: Oscillations of a monsoon system. Part I. Observational aspects. *J. Atmos. Sci.*, **33,** 1937–1954.

Lau, K.-M., and P. H. Chan, 1986: Aspects of the 40–50 day oscillation during the northern summer as inferred from outgoing longwave radiation. *Mon. Wea. Rev.*, **114,** 1354–1367.

Lawrence, D. M., and P. J. Webster, 2001: Interannual variations of the intraseasonal oscillation in the South Asian summer monsoon region. *J. Climate*, **14,** 2910–2922.

Mooley, D. A., and J. Shukla, 1987: Characteristics of the westward-moving summer monsoon low pressure systems over the Indian region and their relationship with the monsoon rainfall. Center for Ocean-Land-Atmosphere Interactions Report, University of Maryland. [Available from COLA, IGES, 4041 Powder Mill Road, Suite 302, Calverton, MD 20705, USA.]

Moron, V., R. Vautard, and M. Ghil, 1998: Trends, interdecadal and interannual oscillations in global sea-surface temperatures. *Climate Dyn.*, **14,** 545–569.

Palmer, T. N., 1994: Chaos and predictability in forecasting the monsoons. *Proc. Indian Natl. Sci. Acad.*, **60A,** 57–66.

Plaut, G., and R. Vautard, 1994: Spells of low-frequency oscillations and weather regimes in the Northern Hemisphere. *J. Atmos. Sci.*, **51,** 210–236.

Pratt, R. W., 1976: The interpretation of space-time spectral quantities. *J. Atmos. Sci.*, **33,** 1060–1066.

Sikka, D. R., and S. Gadgil, 1980: On the maximum cloud zone and the ITCZ over Indian longitudes during the southwest monsoon. *Mon. Wea. Rev.*, **108,** 1840–1853.

Singh, S. V., R. H. Kripalani, and D. R. Sikka, 1992: Interannual variability of the Madden-Julian oscillations in Indian summer monsoon rainfall. *J. Climate*, **5,** 973–978.

Sperber, K. R., J. M. Slingo, and H. Annamalai, 2000: Predictability and the relationship between subseasonal and Interannual variability during the Asian summer monsoon. *Quart. J. Roy. Meteor. Soc.*, **126,** 2545–2574.

Wheeler, M., and G. N. Kiladis, 1999: Convectively coupled equatorial waves: Analysis of clouds and temperature in the wavenumber-frequency domain. *J. Atmos. Sci.*, **56**, 374–399.

Yasunari, T. (1979): Cloudiness fluctuations associated with the northern hemisphere summer monsoon. *J. Meteor. Soc. Japan*, **57,** 227–242.

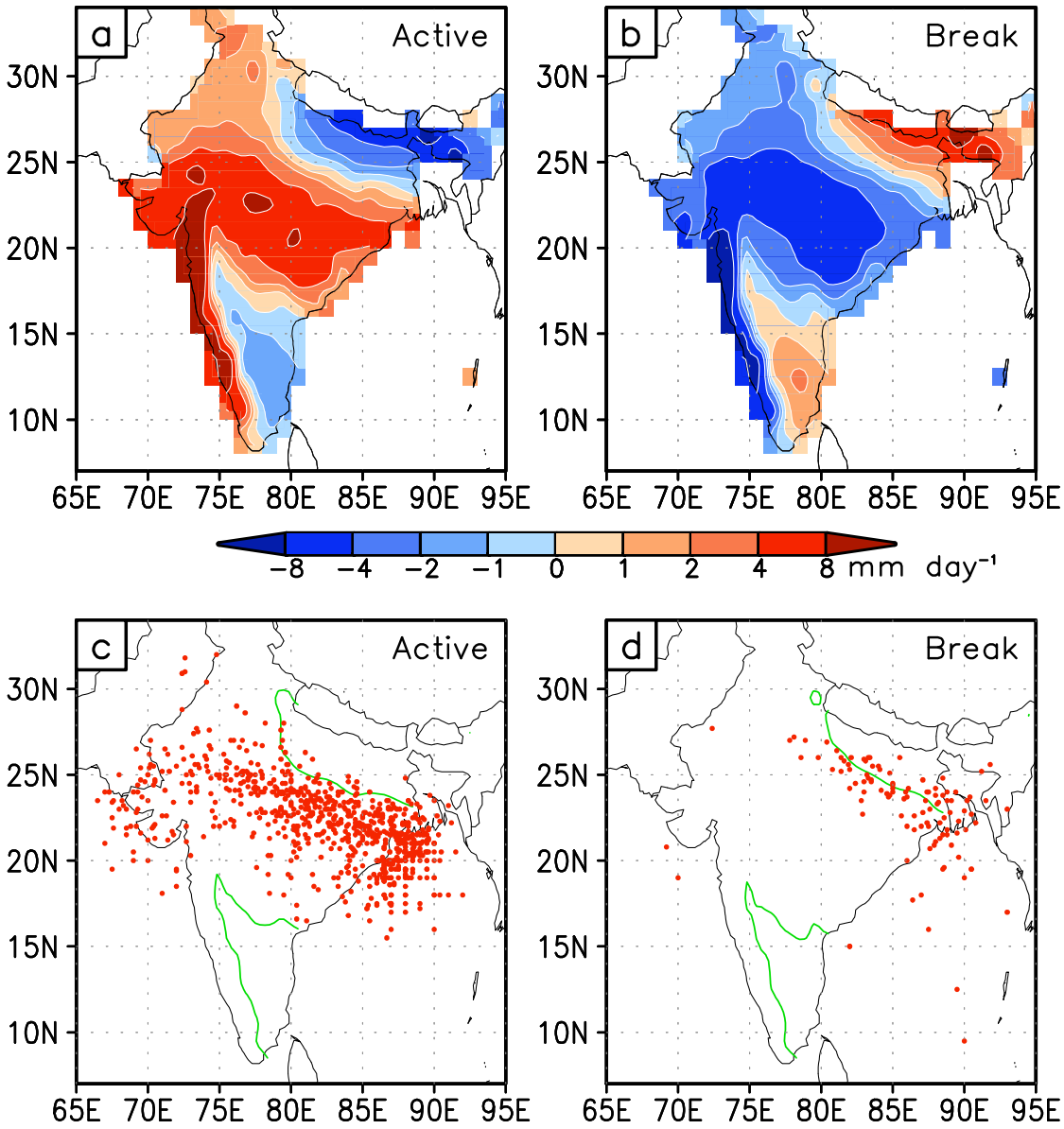

Fig. 1. Active phase composite (a) and break phase composite (b) of daily rainfall anomalies (mm day^{-1}). Active phase composite (c) and break phase composite (d) of depression-days. Each dot in (c) and (d) represents the location of the depression for a day (or depression-day). The zero contours of rainfall in (a) and (b) are plotted in green in (c) and (d), respectively, to indicate the rainfall zones. The composites were constructed for JJAS 1901–70.

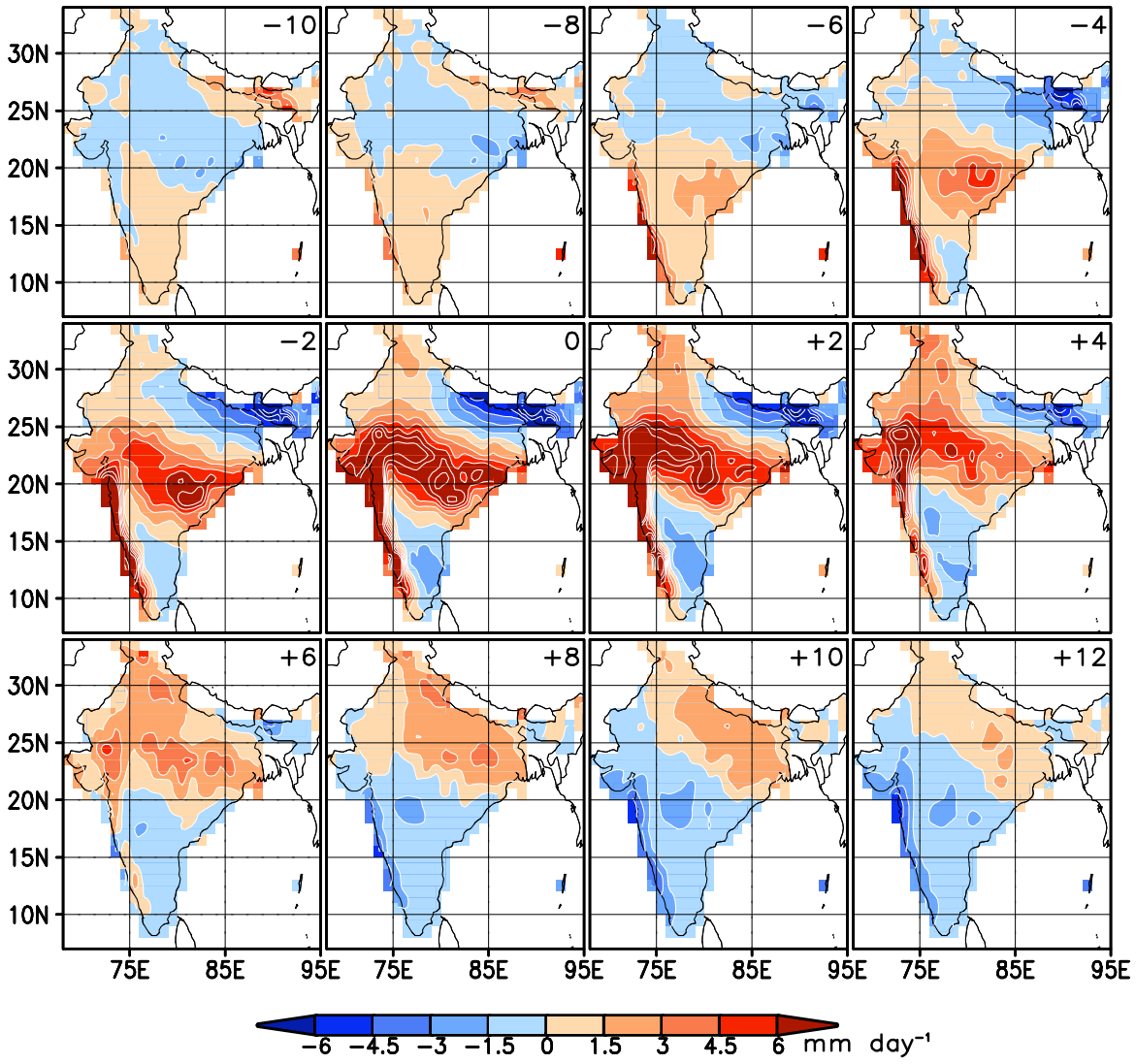

FIG. 2. Lagged active phase composites of daily rainfall anomalies (mm day^{-1}) for JJAS 1901–70. Lag (−) or lead (+) day is indicated at the top right corner of each panel. Lag 0 corresponds to the midpoint of each active phase.

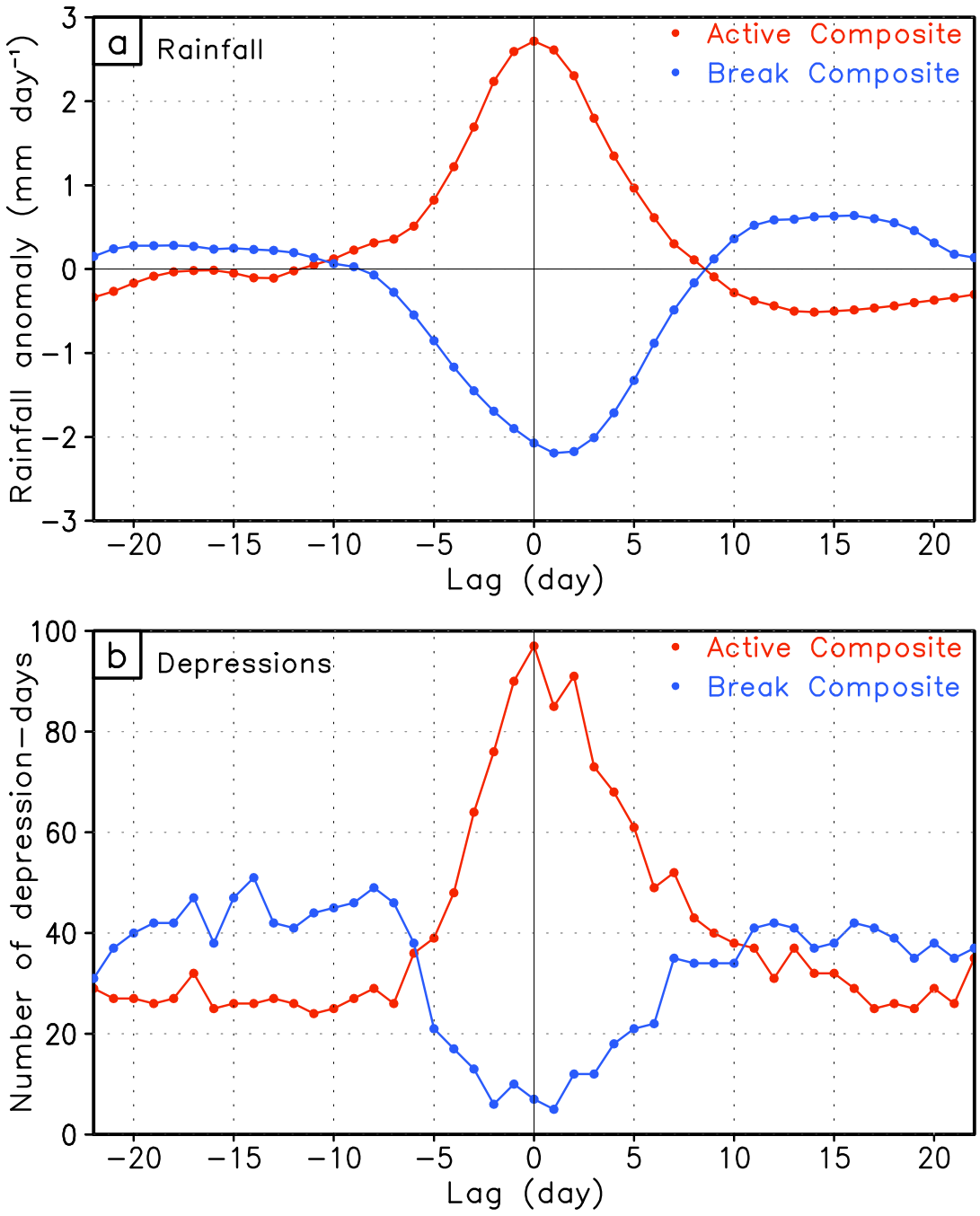

FIG. 3. Lagged active phase composites (red) and lagged break phase composites (blue) of IMR index in mm day^{-1} (a) and depression-days (b) for the period JJAS 1901–70. Lag 0 corresponds to the midpoint of each active or break phase.

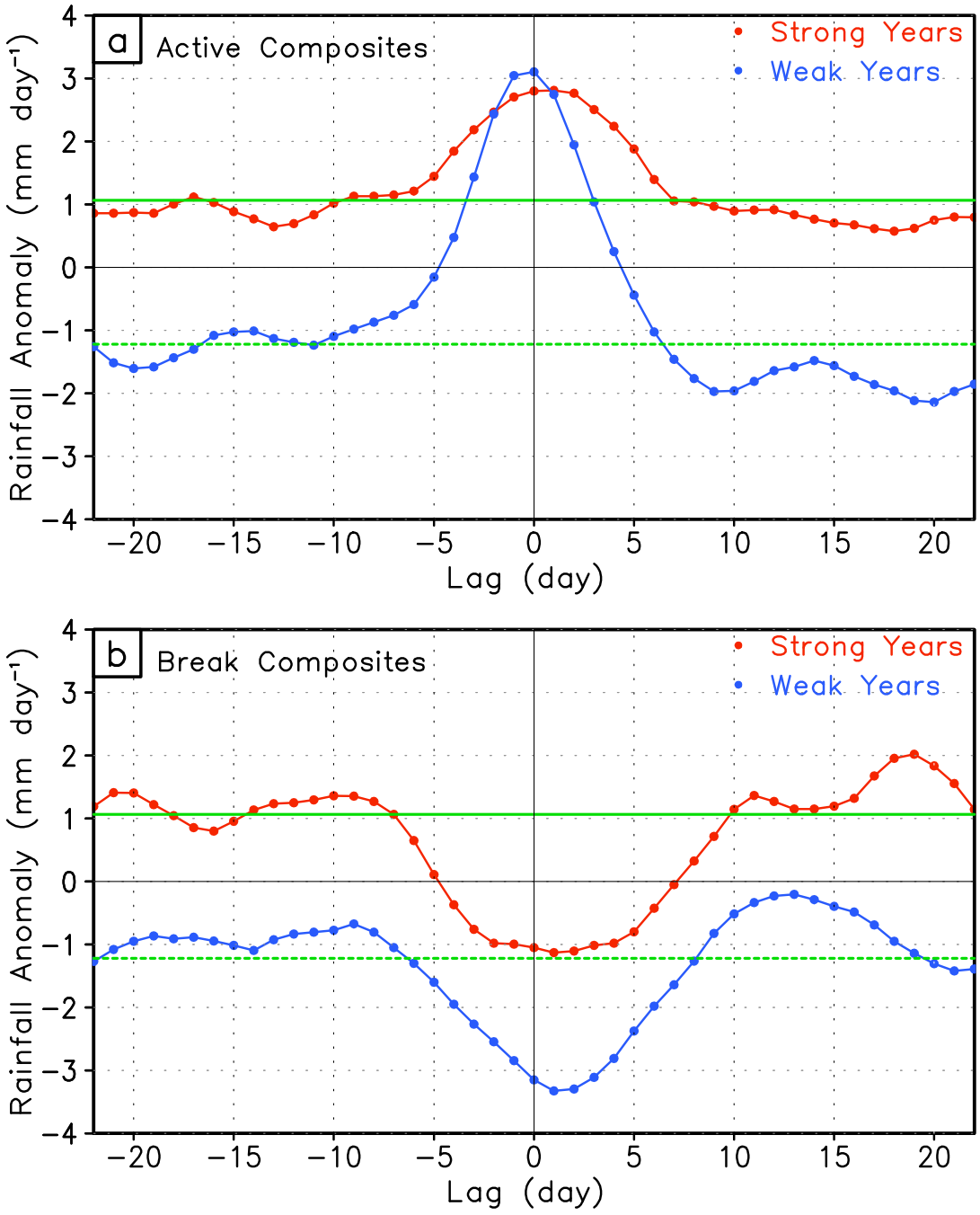

FIG. 4. Lagged active phase composites (a) and lagged break phase composites (b) of the IMR index (mm day^{-1}) during strong monsoon years (red) and weak monsoon years (blue) for the period 1901–70. Lag 0 corresponds to the midpoint of each active or break phase. The solid (dashed) green lines represent the JJAS seasonal mean IMR index averaged over strong (weak) monsoon years.

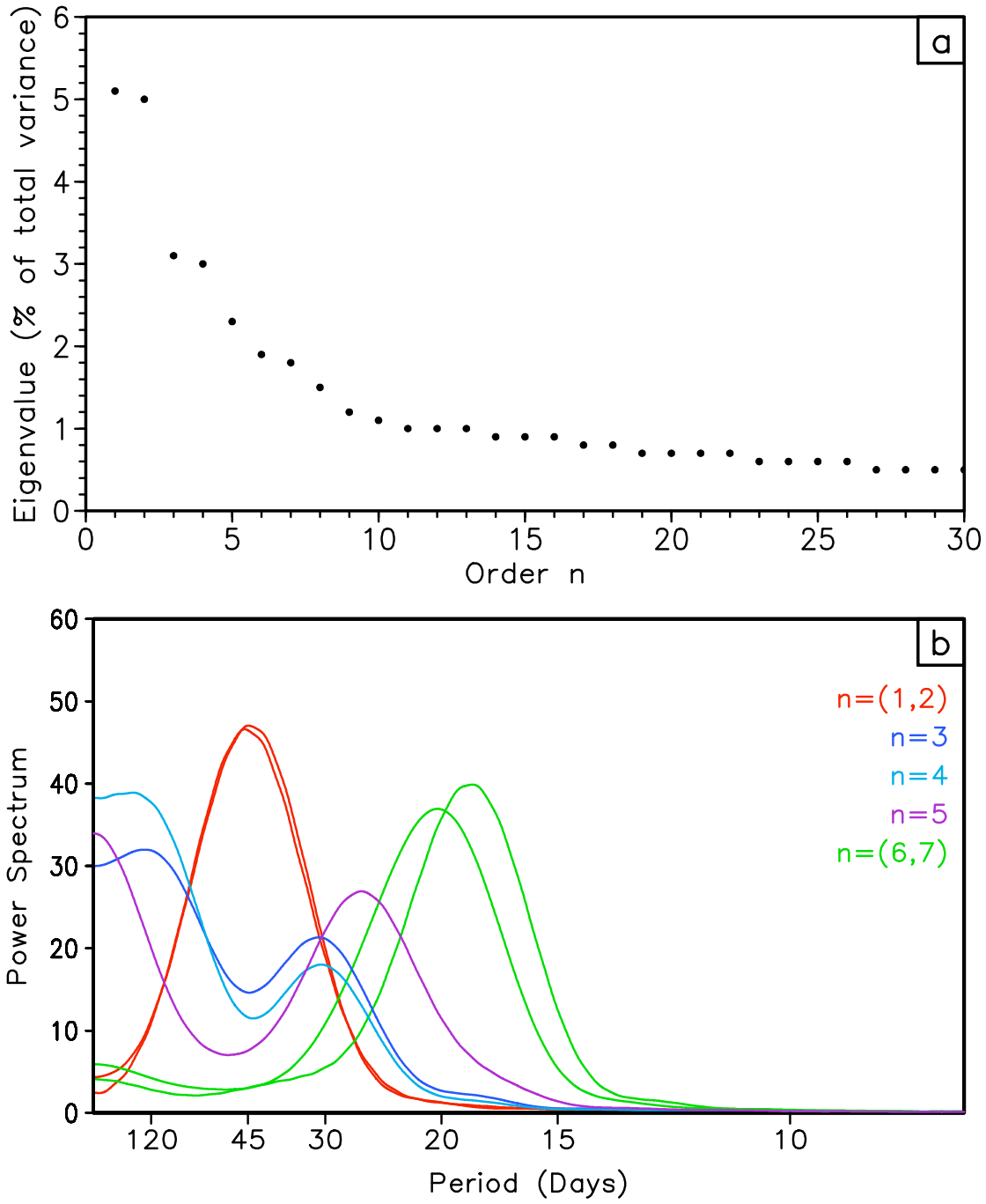

FIG. 5. MSSA of daily rainfall anomaly for JJAS 1901–70: (a) Eigenvalue spectrum with the first 30 eigenvalues plotted as percentage of the total variance, and (b) power spectra of the first seven PCs.

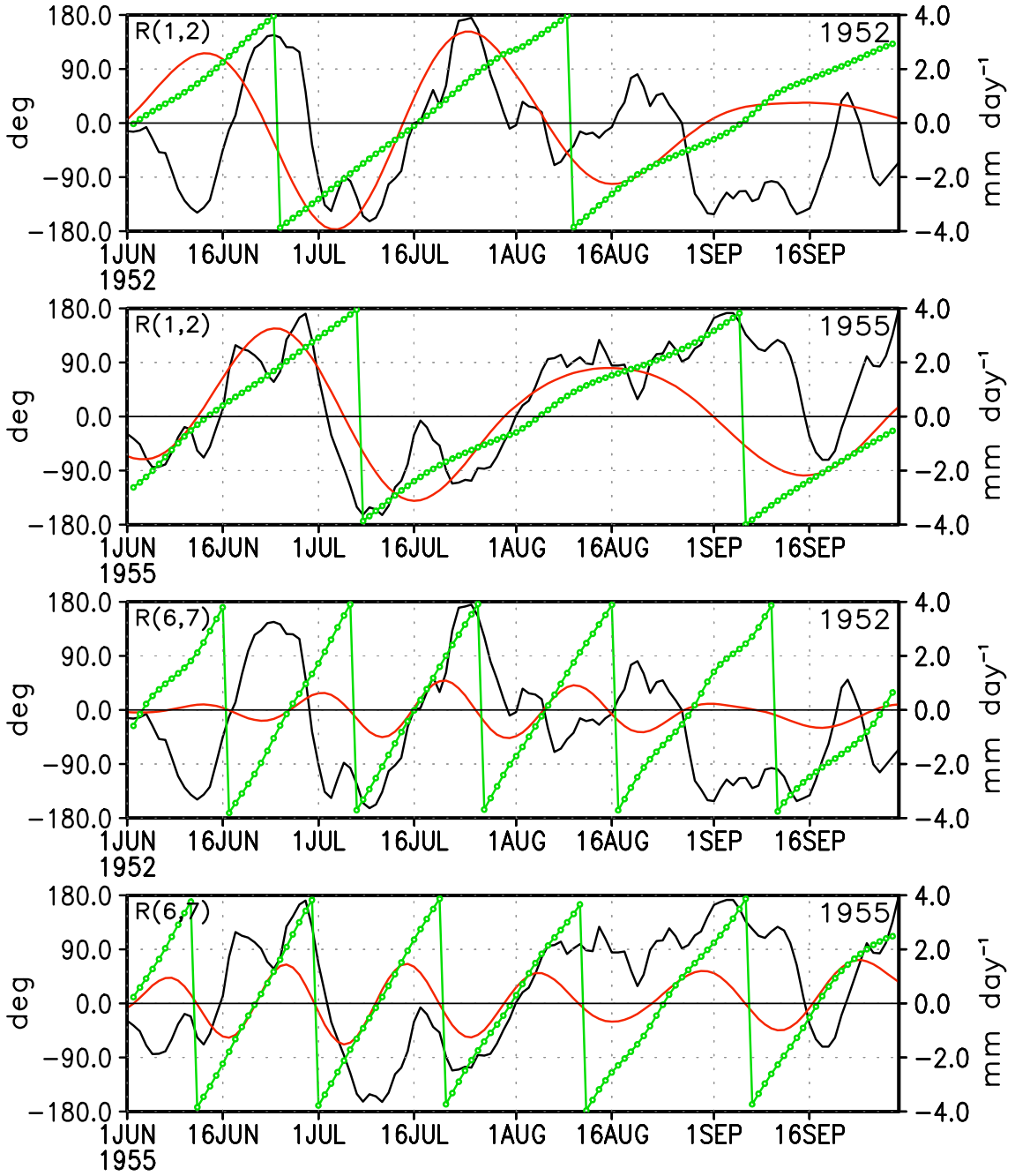

FIG. 6. Time series of daily IMR index (solid black), phase angle of daily RCs (green circle) and the RCs (red) at grid point (77°E, 20°N) for JJAS of 1952 and 1955. $R(1,2)$ is plotted in the top two panels and $R(6,7)$ in bottom two panels. The year is indicated at the top right corner. The scale for the phase angle of the RCs in degrees is at left and the scale for the IMR index and the amplitude of the RCs in mm day^{-1} is at right.

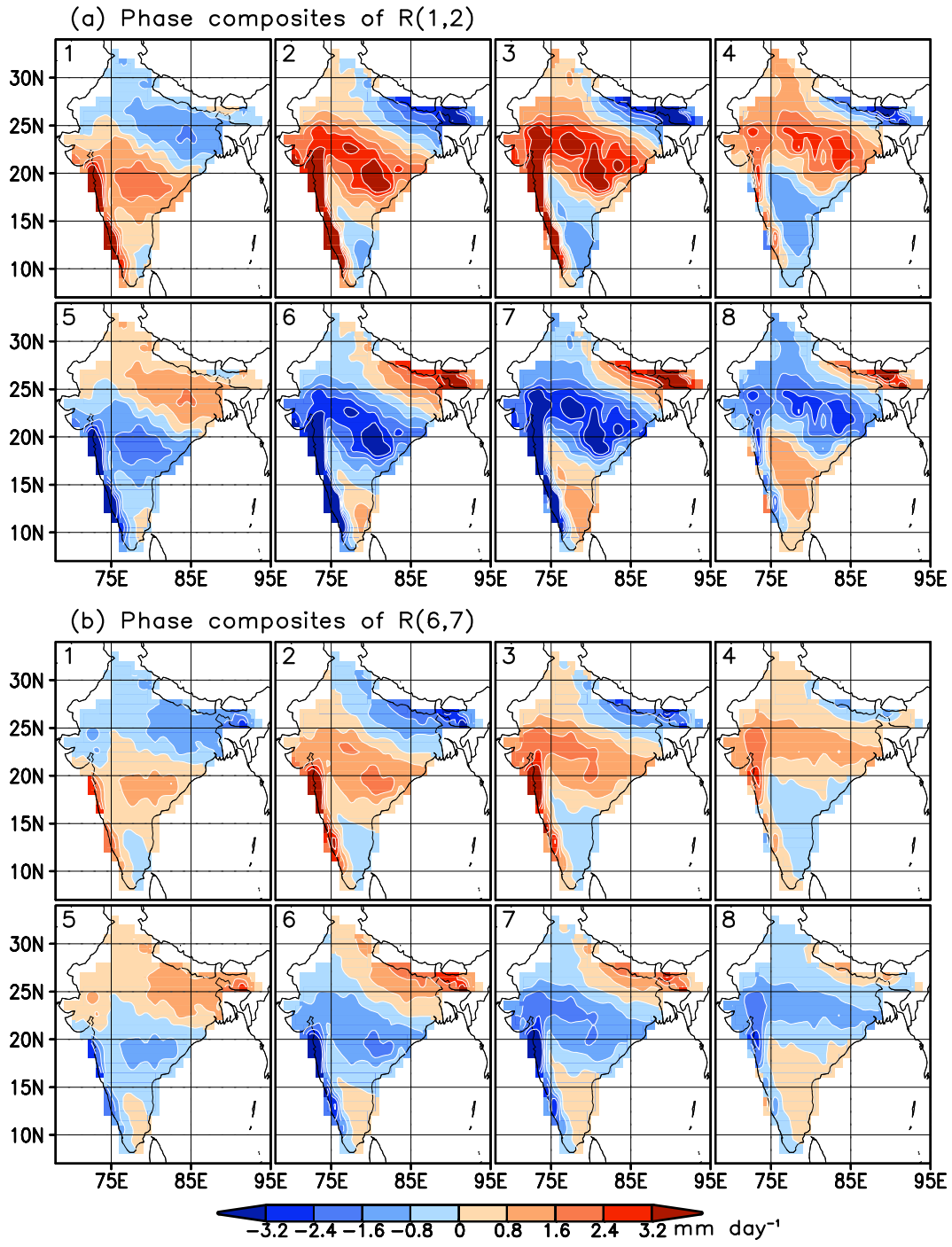

FIG. 7. (a) Phase composites of $R(1,2)$ of the oscillation 1–2 with a period of about 45 days and (b) phase composites of $R(6,7)$ of the oscillation 6–7 with a period of about 20 days. Units are in mm day^{-1}. The phase number is given at the top left corner of each panel.

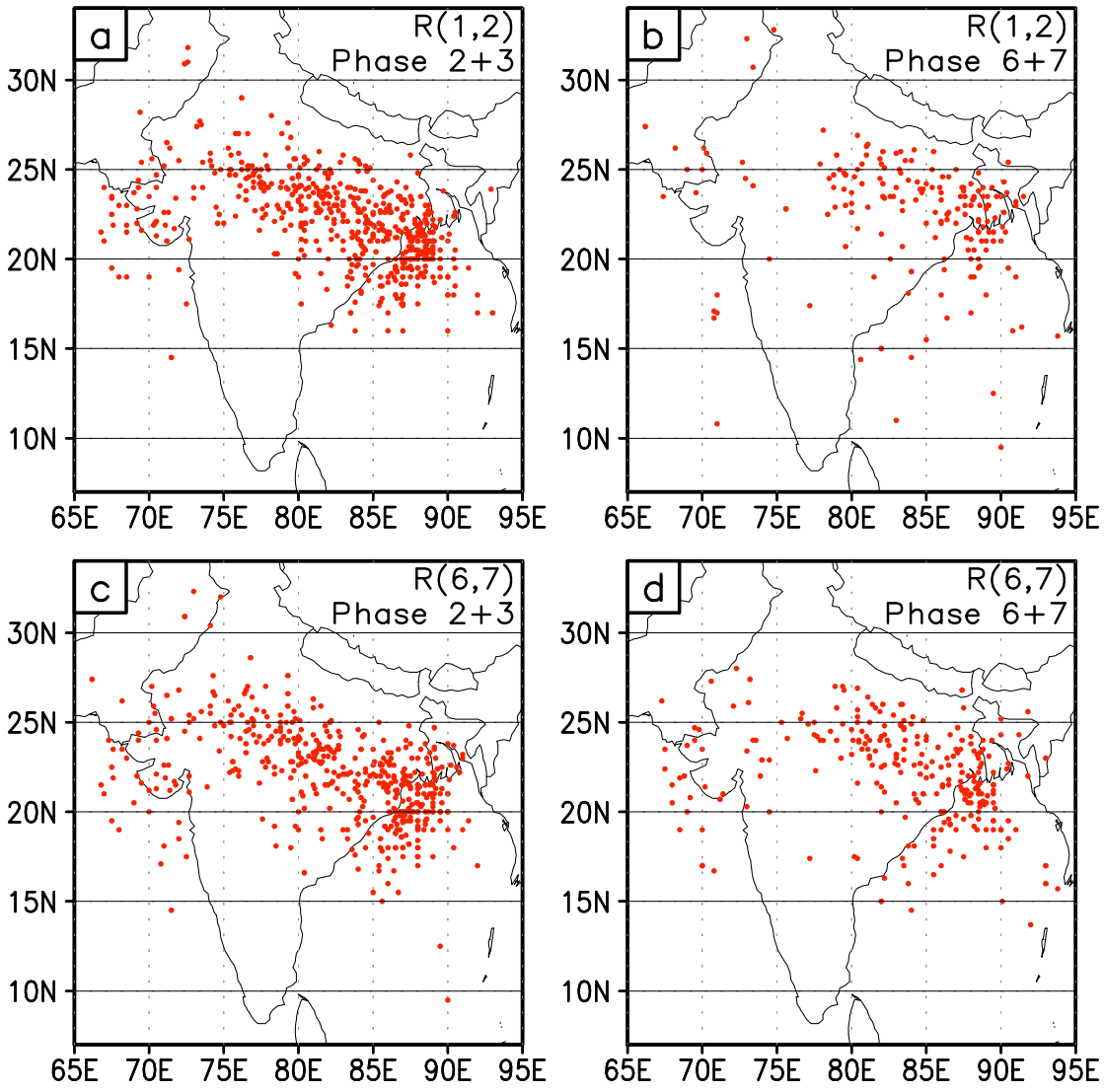

FIG. 8. Phase composites of depression-days for (a) combined phases 2 and 3 and (b) combined phases 6 and 7 of the oscillation 1–2. Phase composites of depression-days for (c) combined phases 2 and 3 and (d) combined phases 6 and 7 of the oscillation 6–7. The phases are the same as those in Fig. 7. Each dot represents the location of the depression for a day.

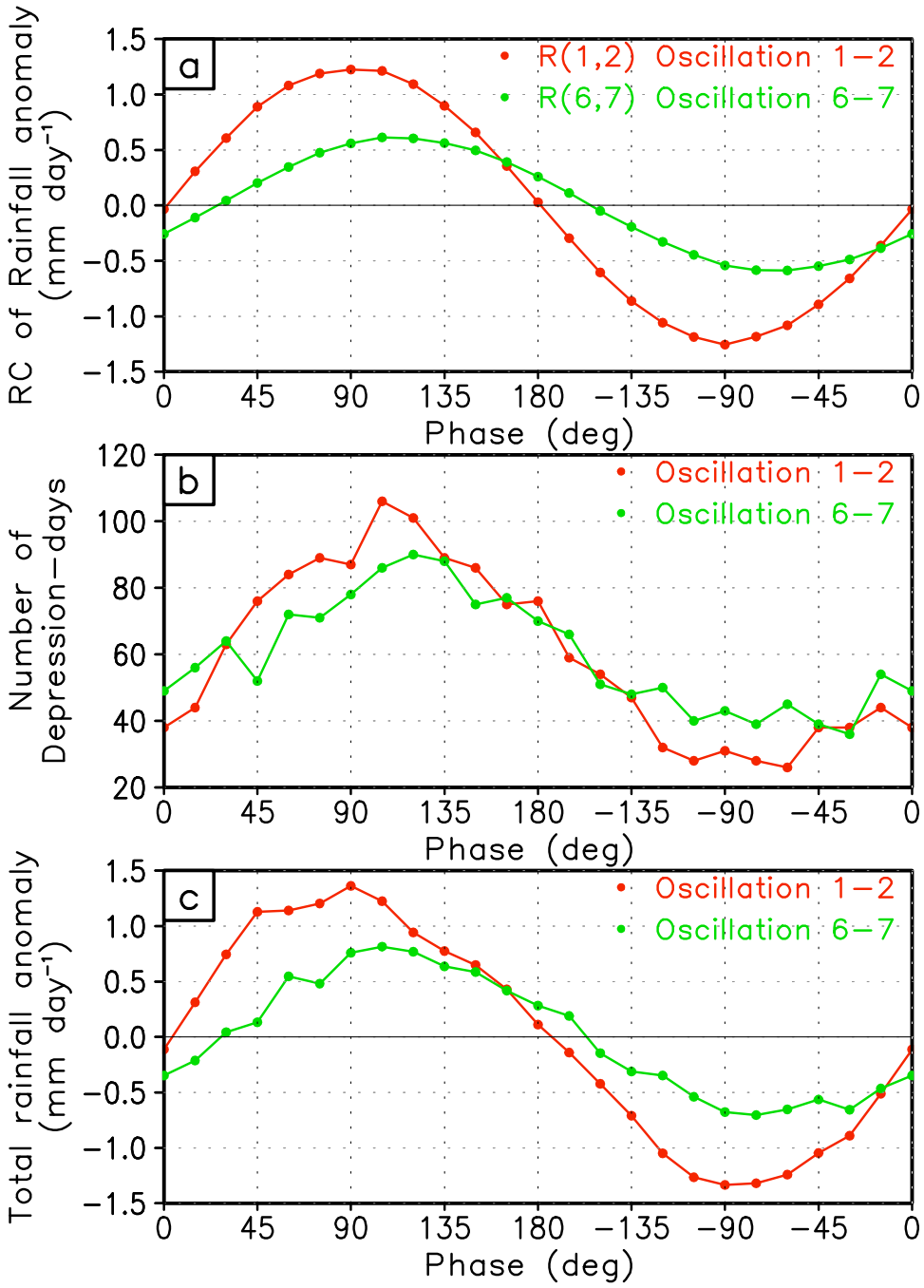

FIG. 9. Phase composites of (a) $R(1,2)$ and $R(6,7)$ in mm day^{-1} (b) depression-days and (c) total rainfall anomalies in mm day^{-1} for oscillations 1–2 (red) and 6–7 (green). The composites were constructed for phase intervals of 15 degrees during JJAS 1901–70.

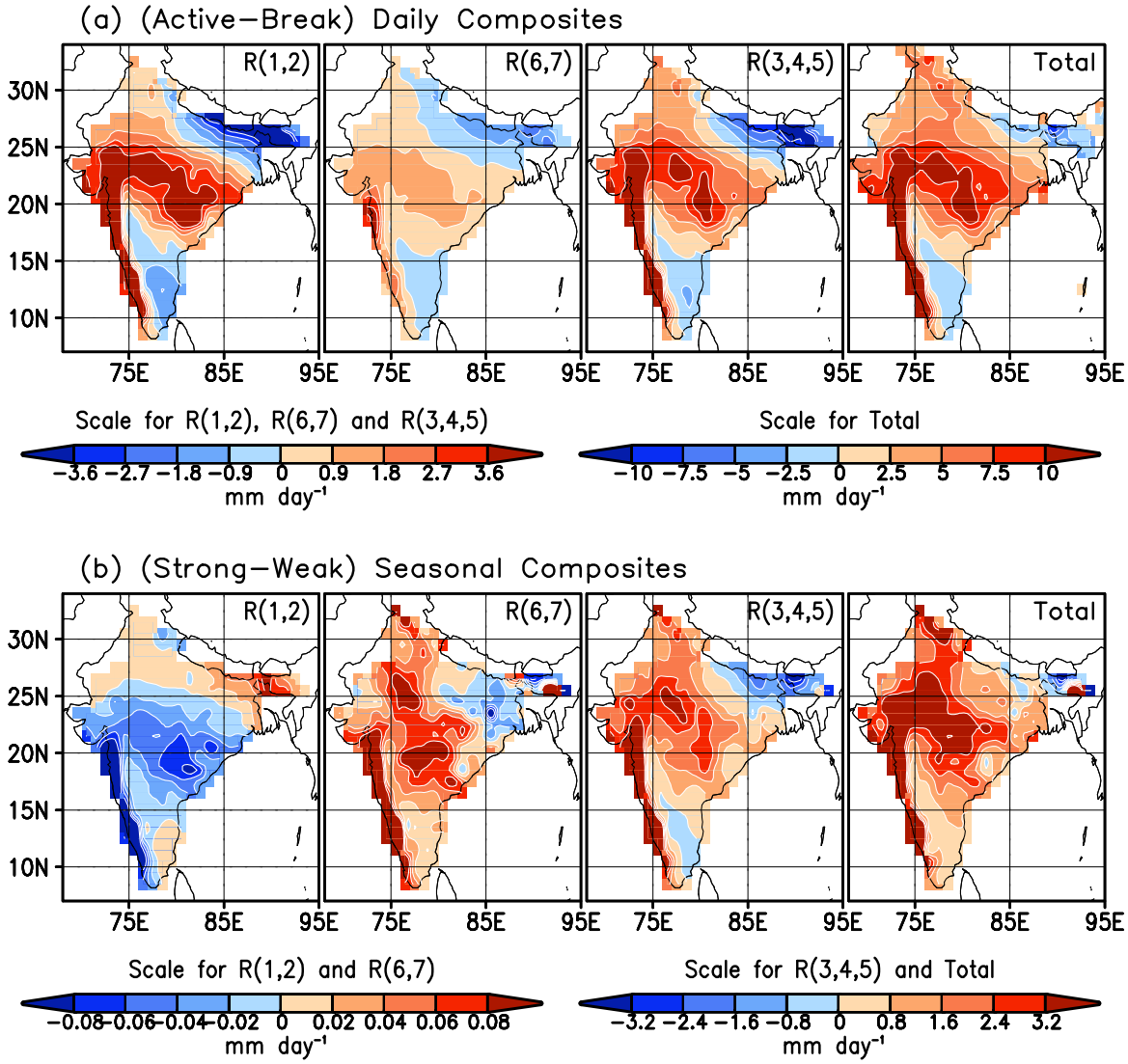

FIG. 10. (a) Difference between active phase composite and break phase composite of daily RCs and daily total anomalies and (b) difference between strong monsoon year composite and weak monsoon year composite of seasonal mean RCs and seasonal total rainfall anomalies. The components plotted are identified at the top right corner. Note the different contour scales.

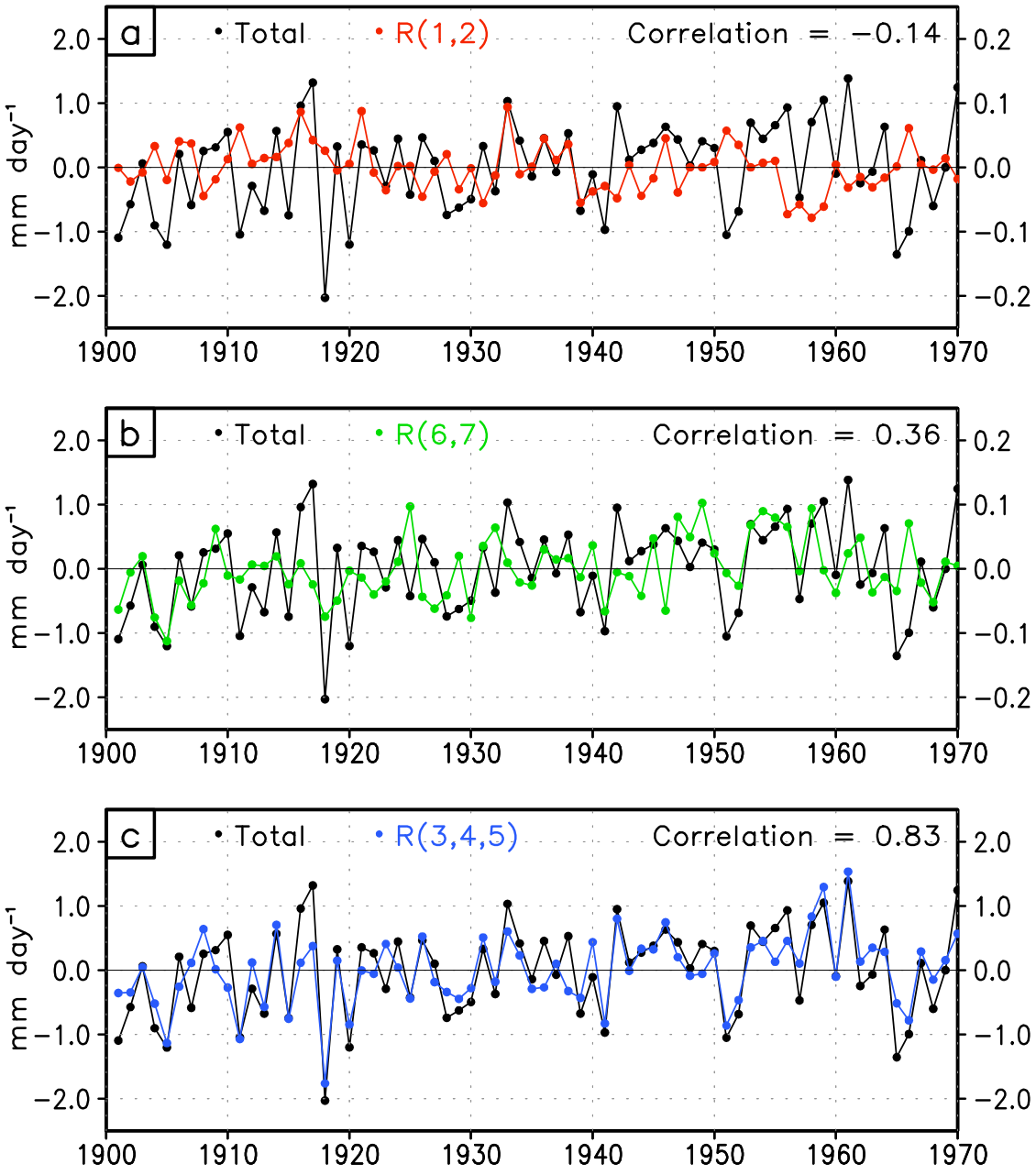

FIG. 11. Time series of JJAS seasonal mean of (a) $R(1,2)$ (red) (b) $R(6,7)$ (green) and (c) $R(3,4,5)$ (blue) area averaged over India. The time series of total rainfall anomaly (i.e., JJAS seasonal IMR index) is plotted in black in each panel for comparison. The scale for the total anomaly is given at left and that for the RCs is at right. The correlation between the total anomaly and the RC plotted in each panel is given at top right corner.

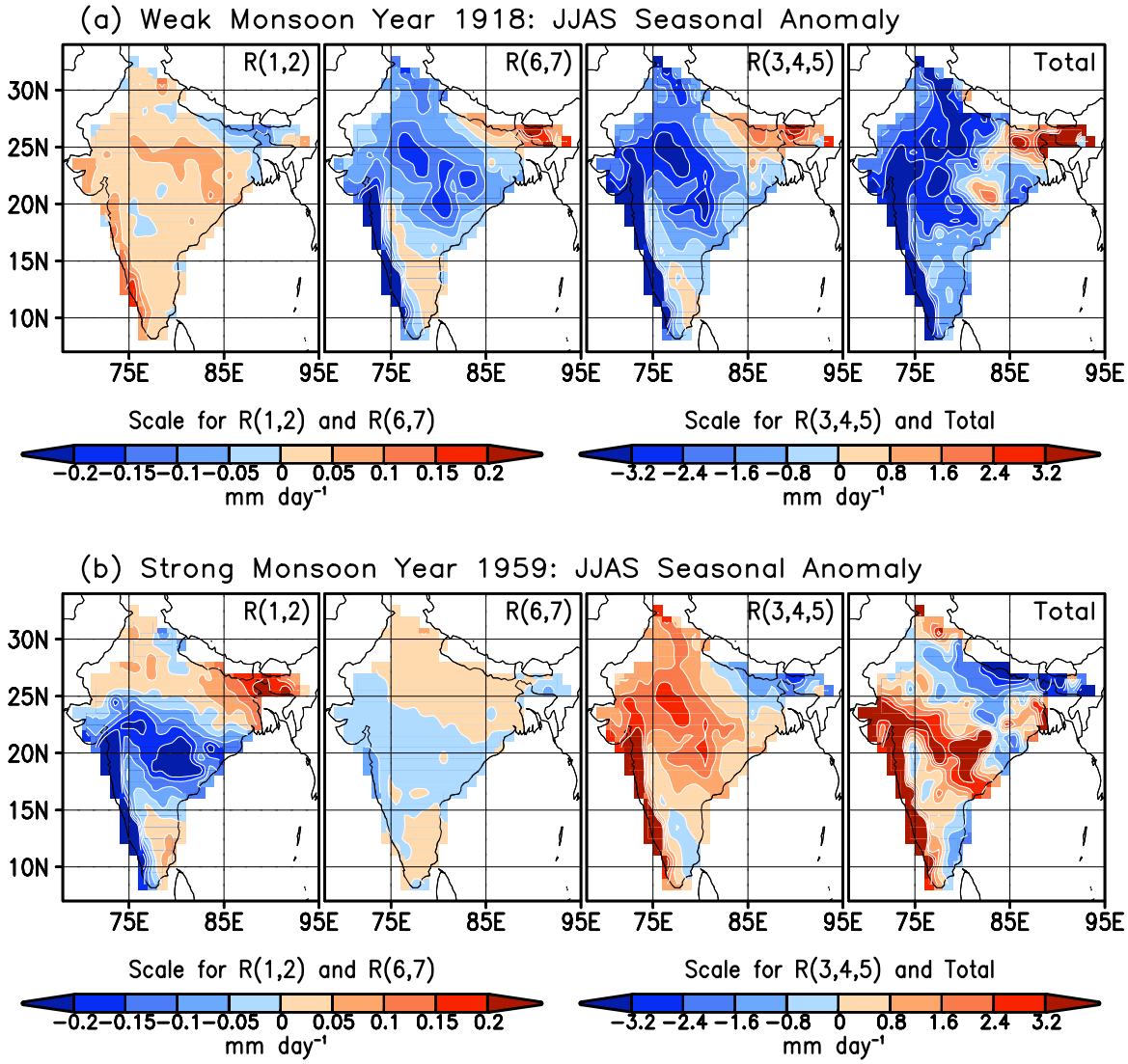

FIG. 12. JJAS seasonal means of total rainfall anomaly and RCs for (a) weak monsoon year 1918 and (b) strong monsoon year 1959. Units are in mm day^{-1}. The components plotted are identified at the top right corner.

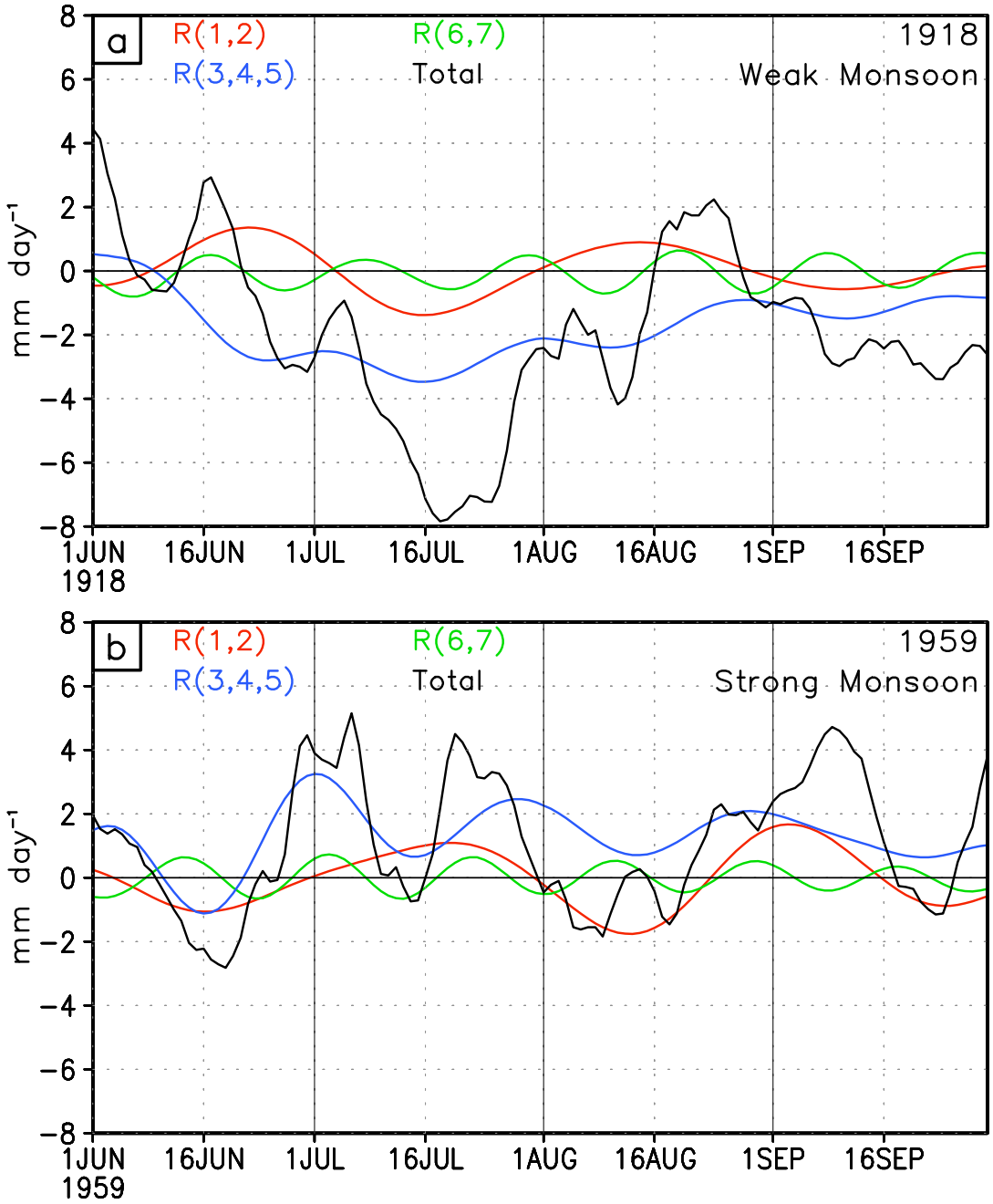

FIG. 13. Time series of daily total rainfall anomaly (black), $R(1,2)$ (red), $R(6,7)$ (green) and $R(3,4,5)$ (blue) area averaged over India for JJAS of (a) weak monsoon year 1918 and (b) strong monsoon year 1959.

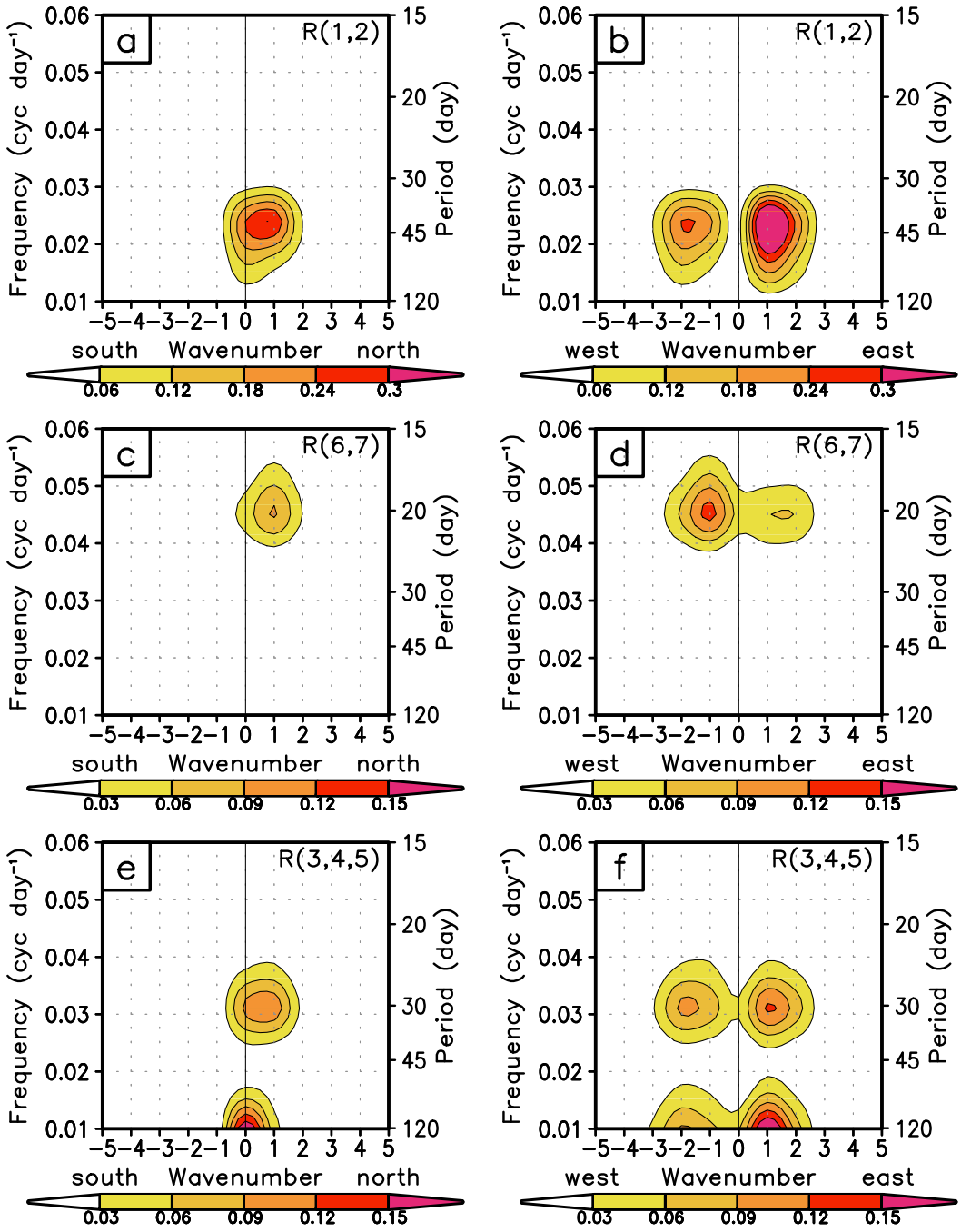

FIG. 14. Wavenumber-frequency spectra from latitude-time domain of (a) $R(1,2)$, (c) $R(6,7)$ and (e) $R(3,4,5)$ and from longitude-time domain of (b) $R(1,2)$, (d) $R(6,7)$ and (f) $R(3,4,5)$ for JJAS 1901–70. The frequency scale is at left and the period scale at right.